Unsteady aerodynamic forces on long lorry platoons

Robertson, Francis; Soper, David; Baker, Christopher

DOI:
10.1016/j.jweia.2020.104481

Document Version
Peer reviewed version

Citation for published version (Harvard):
Robertson, F, Soper, D & Baker, C 2021, 'Unsteady aerodynamic forces on long lorry platoons', *Journal of Wind Engineering and Industrial Aerodynamics*, vol. 209, 104481. https://doi.org/10.1016/j.jweia.2020.104481

Unsteady aerodynamic forces on long lorry platoons

F. H. Robertson, D. Soper, C. Baker
School of Engineering, University of Birmingham, Edgbaston, Birmingham, United Kingdom
B15 2TT

Abstract

In an earlier paper the authors describe an experimental investigation to measure the forces on 1/20th scale vehicles in long platoons, together with the flow field around the platoons, using the University of Birmingham moving model TRAIN rig facility, that can accommodate 8-vehicle platoons and provide a realistic ground simulation. This paper analyses the experimental results further to look at the unsteady forces and flows. Using conventional Fourier spectral analysis and wavelet analysis, it is found that there are two modes of unsteady flow – one at a low frequency that affects multiple vehicles in the platoon at any one time, and has a wavelength of several vehicle lengths; and one at a high frequency with a much shorter wavelength that is localised on specific vehicles. These flows are very intermittent and unsteady, with switching between modes both spatially and temporally. Associated DDES calculations only capture the low frequency mode. Scaling up the measured values to the full-scale situation gives values of the standard deviation of side force on an individual lorry of around 260N, with the major frequency of oscillation at 1.0Hz.

Keywords: Vehicle aerodynamics; lorry; platoon; lateral stability, slipstream; moving model.

1. Introduction

The aerodynamics of isolated road vehicles has been extensively studied in recent decades, with the main aim of reducing the aerodynamic drag of vehicles, to decrease fuel consumption; although other effects such as wake flows, cross wind stability, water spray and soiling effects etc have also been studied (see for example Schuetz, 2015). However, much less work has been directed towards the interactions between vehicles, and particularly vehicles that run in close proximity in streams of traffic, either informally, or more formally as vehicle platoons. It is with the latter that this paper is concerned.

There has been some recent work to investigate the aerodynamics of platoons including full-scale field tests (CORDIS, 2012; Chan, 2012; Davila et al, 2013; Ebrahim, 2018), scale-model laboratory testing (Zabat et al, 1995; Tsuei & Savaş, 2001; Robertson et al, 2019; Le Good et al, 2018; Watkins and Vino, 2008; Pagliarella et al, 2007) and Computational Fluid Dynamics (CFD) (Davila et al, 2013; He, et al, 2019; Vegendla et al, 2015; Humphreys and Bevly, 2016; Mirzaei and Krajnović, 2016; Bruneau et al, 2017; Ebrahim and Dominy, 2020). This work has also focused on changes to the mean drag force of vehicles in platoons. Most of these tests were carried out with relatively short vehicle platoons (three or four vehicles maximum), and the physical model tests sometimes used static models in wind tunnels with what were unrealistic ground simulations. To overcome these issues, Robertson et al (2019) recently conducted moving model experiments with a long 1/20th scale eight-lorry platoon on a moving model rig, with a correct ground simulation, at vehicle spacings from 0.5 to 1.5 vehicle lengths. Substantial reductions in aerodynamic drag were measured for the non-leading platoon vehicles with drag coefficients plateauing towards the rear of the platoon. The drag decreased with spacing, with a 57% reduction for the closest spacing. Drag results for the same platoon configuration, obtained via Delayed Detached Eddy Simulation (DDES), were in excellent agreement with the experimental results (He et al, 2019). This reduction in aerodynamic drag is perhaps the major advantage of platooning given the increasing demand for more environmentally friendly transport systems and global needs for decarbonisation. For example, the EU has set a target to reduce the total greenhouse gas emissions to 5-20% of the 1990 levels by 2050 (Davila et al , 2013). The full scale experiments of SATRE concluded that the equivalent savings of CO_2 per year could be up to 2.8 and 0.1 tons for trucks and cars respectively (CORDIS, 2012; Davila et al, 2013) with the largest reductions achieved with smaller inter-vehicle spacing.

Now recent advances in technology such as digital mapping, position recognition and inter-vehicle communications have the potential to revolutionise vehicle design and operation, through the development of autonomous road vehicles (AVs) (Iliaifar, 2013). It is fair to say that there is much scepticism concerning whether or not AVs will be introduced in the short or medium term, and the technical and social challenges to their use are immense. Nonetheless in principle, AVs can potentially drive safely in proximity, in platoon formation, thus improving the efficiency of road use (Goldin, 2018). Several projects have trialled partially self-driving vehicles in platoon on test tracks and major public roads in countries including Germany, the USA and Japan (BBC News, 2017). SARTRE (Safe Road Trains for the Environment), a project by companies from four countries within the European Union, successfully tested a platoon consisting of 2 trucks followed by 3 cars (CORDIS, 2012; Chan, 2012; Davila et al, 2013). Additionally, the TRL (Transport Research Laboratory) are overseeing tests with 3 lorries in the UK's first heavy goods vehicle platooning trial (BBC News, 2017; DfT, 2017). Some estimates suggest that AVs could be commercially available as early as 2025

(Fallah, 2018) and that the economic benefits could be up to $1.9 trillion per year (Manyika et al, 2013).

Now whilst the potential drag benefits for lorry platoons are well established, the unsteady forces arising from running vehicles in close formation are less well understood. Frequency analysis of wake velocity or base pressure measurements is commonly used to investigate coherent structures emanating from and oscillating forces on a single vehicle (Grandemange et al, 2013; Lahaye et al, 2014; Volpe et al, 2015; Mcarthur et al, 2018) but such analysis is largely overlooked for vehicle platoons. Unsteady sideways forces are of course particularly important as the overall stability of vehicles may be compromised. Significant effects on vehicle handling have been observed in stock car racing when one car travels in the wake of another (Katz, 2016). Similarly, the simulations by Humphreys and Bevly (2016) showed that the trailing vehicle in a two-truck platoon experienced buffeting, presumably due to vortices shed by the front vehicle. The DDES results on the eight-lorry platoon mentioned above (He et al, 2019) suggested that lorries in platoons could experience significant oscillating lateral forces, which increased along the platoon.

This paper considers this issue and in particular looks at unsteady lateral forces on lorries in platoons, and the unsteady nature of the flow field around them, using the experimental data from the investigations of Robertson et al (2019) and, to a limited extent, the computational data of He et al (2019) described above. The objectives of this investigation were:

- to analyse the experimental data to determine if any significant lateral oscillations could be detected and,
- if such oscillations were present, to quantify both their frequency and their magnitude at model scale and to estimate full scale values.

It will be seen that such oscillations were found, but they were highly complex and intermittent in nature, and a number of novel analytical techniques had to be used to fully describe them.

The experimental and analysis methodology is considered in section 2. Section 3 describes the results of a spectral analysis of lateral vehicle forces on the lorries in the platoon, and section 4 describes a wavelet analysis of the transient flow around the side of the vehicle. The nature of the flow around the vehicle is discussed in section 5, and conclusions are set out in section 6.

Note that during the overall project from which the current results are taken, platoons of Windsor vehicles and railway trains running close together were also studied. These results will be published in due course.

2. Methodology

2.1 Experiment Methodology

The experiments were conducted at the University of Birmingham Transient Aerodynamic Investigation (TRAIN) rig facility. This is a moving-model facility, which is ideal for examining the transient aerodynamics of moving vehicles as it correctly models the relative movement of vehicles with respect to the ground (Baker et al, 2001). The experimental platoon consisted of eight 1/20th scale model lorries manufactured from Glass Reinforced Plastic (GRP). The models are based on a Leyland DAF 45-130, with detailed components such as wing mirrors or underbody skirts either simplified or removed. The chosen number of vehicles was designed to ensure a well-developed boundary layer, estimated based on prior aerodynamic knowledge (Soper et al, 2014), and to maximise the capabilities of the moving model facility. The model platoon was propelled along a 150 m long track using an elastic bungee propulsion system. A 20 m long suspended ground plane was erected over part of the track, to simulate road conditions, at a position on the rig which was suitable to ensure that the model vehicles were travelling at a stable speed. The vehicles were mounted onto a long spine that ran through a slot in the middle of the ground plane to ensure the vehicles travelled with a constant spacing between them. The mounting method allowed the vehicles to be freely moved along the spine. Normalised spacings s of 0.5, 1.0 and 1.5 vehicle lengths (where the vehicle length L = 0.395m) were tested. The platoon lengths (L_p) for the three cases are 4.54m, 5.92m and 7.31m respectively. A photograph of the experimental set up is given in Figure 1.

A series of photoelectric position finders were set up along the ground plane within the 4 m test section towards the downwind end of the ground plane. The speed was calculated from the time taken for the first lorry to break consecutive beams. The average vehicle speed for all runs was V = 25 ± 1 m/s; close to the maximum speed achievable with the TRAIN rig setup due to the significant weight of the platoon. The corresponding Reynolds number, based on the lorry height, is of the order of 3×10^5. A light detector was also installed in each vehicle and the outputted data linked to the other vehicles to synchronise data from each lorry and run of the experiment.

Two sets of measurements were carried out – the measurement of surface pressures on the lorries in the platoon, using transducers that were mounted inside the lorries, and the measurement of slipstreams around the platoon that measured velocities and static pressure as the vehicles passed.

The pressure on the vehicle surfaces was measured at a sampling rate of 3 kHz with a series of bespoke on-board pressure monitoring systems that were built into all vehicles. Reference ports of the internal transducers where connected to a manifold in each vehicle via silicon tubing. These manifolds were connected to a sealed reservoir to synchronise the on-board reference pressure between all vehicles. In total there were 40 pressure tappings on each model, but only 14 could be connected to the transducers at any one time due to space limitations. For each configuration (i.e. one set of tappings and one vehicle spacing) a minimum of 15 runs of the platoon on the rig were conducted, creating a very extensive experimental programme with many hundred individual runs. The data for each lorry and run were initially aligned to where the front lorry reaches the central light gate and cropped with respect to the test section. Pressure was then calculated from the raw voltage data through Betz manometer and tube length correction calibrations. A 5s trace of pressure data, when

the lorries are stationary, is averaged and subtracted from the pressure for each run, to give the differential pressure in relation to the ambient room pressure.

The slipstream development at the side of the platoon was recorded by static multi-hole pressure probes, capable of measuring local static pressure and all three components of velocity. Measurements were made at a sampling frequency of 5 kHz and filtered using a 650 Hz low-pass filter to reflect the maximum frequency response of the probe (Soper et al, 2016). The measurements were made with a series of rakes of probes near the mid-wheel height, mid-vehicle height and just below the top of the vehicle at a number of distances from the vehicle sides. A series of 20 runs were conducted for each measuring position and vehicle spacing and the raw data from each run was aligned with the point at which the leading lorry reached the probes.

Robertson et al (2019) provides further detail on the experimental setup including the equipment specifications, ambient conditions and multi-hole pressure probe and vehicle surface pressure tap positions. For detailed information regarding the TRAIN rig moving-model facility see Soper et al. (2016).

Figure 1. The platoon model on the TRAIN Rig

2.2 Analysis Methodology

The main aim of the current work is to investigate the overall lateral unsteadiness on the vehicle. Ideally the side force would be calculated by area integrating the measured pressures. However, as the number of transducers which would fit inside each lorry was limited, not all tap positions were measured simultaneously. Thus, data will be presented here for the differential pressure between three sets of pressure taps as shown in figure 2. Pair A on the side of the box near the front, and pairs B and C further back. These differential pressures are indicative of the lateral force on the vehicle at different points along the trailer and were chosen to attempt to capture what was thought *a priori* to be the most important flow

features - separation around the front of the trailer, a fluctuating reattachment in the centre of the trailer, and an attached area near the rear. After an initial filtering of the raw pressure data using a 6th order Butterworth filter with a cut-off frequency of 100 Hz, the differential pressure was then formed by subtracting the time series of the pressure on each side of the lorry, and then subtracting the mean of this time series (which was usually small). The pressure was expressed in coefficient form $C_P(\tau) = \frac{\Delta p(\tau)}{\frac{1}{2}\rho V^2}$ where , $\Delta p(\tau)$ is the differential pressure at τ, ρ is the fluid density and V is the speed of the platoon. $\tau = Vt/L$, is the dimensionless time where $t = 0$ is defined as the time at which the front of the first lorry reaches either the start of the test-section or the multi-hole pressure probe for surface pressure and slipstream measurements respectively. For each configuration that was tested (i.e. for each vehicle spacings *s*, and each set of tapping positions), the variance of the coefficient ${\sigma_{Cp}}^2$ (the square of the standard deviation) was calculated and the power spectral density S_{Cp} found using conventional Fourier analysis. The original intention had been to then average the spectra using the technique of ensemble averaging for each configuration. However, it will be seen that this proved to be inappropriate and most of the analysis focussed on individual spectra. Frequencies were also put into the non-dimensional form $F = \frac{fW}{V}$ where *f* is frequency and *W* is the lorry width (= 0.125m).

For some lorries, the pressures at tapping pairs A, B and C were measured simultaneously, and thus an estimate of the overall side force coefficient on the lorry box could be determined by taking the area weighted average of the fluctuating pressure time series at the tapping pairs.

Wavelet analysis has been carried out to investigate the unsteady behaviour of the platoon slipstream and to relate these to the unsteady pressures. Wavelet transforms are ideally suited to analyse the frequency content of a transient signal as a function of time (Baker et al, 2001). A summary of wavelet analysis is given by Torrence and Compo (1998) and the analysis has been conducted using the online software that they provide. In what follows we will use the velocity time series measured at 0.08 m above ground level and 0.025 m from the lorry side (figure 3). The input signal is the filtered, normalised longitudinal velocity from a single run without resampling. The mother wavelet is a Morlet, as has been used previously in vehicle aerodynamics studies investigating the slipstream and wakes of high-speed trains (Soper et al, 2014). This procedure gives a contour plot of wavelet power against wavelet scale and dimensionless time $\tau = Vt/L$. Again, individual rather than averaged wavelet plots will be mainly considered.

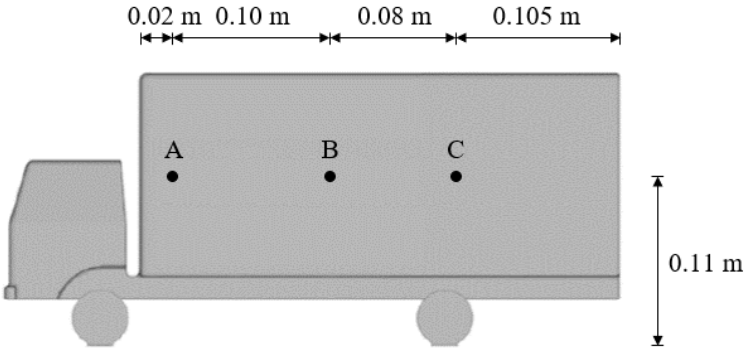

Figure 2. Pressure tap positions.

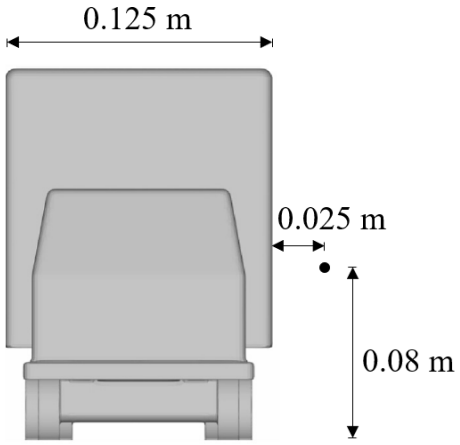

Figure 3. Slipstream velocity measurement position

3. Analysis of pressure spectra

3.1 Preliminary observations and categorisation of spectra

The initial approach to analysing the data was to attempt to carry out an ensemble analysis of the differential pressure coefficient spectra i.e. the averaging of all spectra for a specific vehicle, spacing and tapping position. This analysis proved to be inconclusive with no clear trends emerging when different spacings and tapping positions were considered. Further investigation showed that the differential spectra, even for a specific vehicle spacing and tapping position, could vary significantly from run to run. After inspection of a wide range of different spectra it was found that three distinct types could be identified. Examples of these are shown in figure 4, which show plots of the normalised spectra $S_{Cp}/{\sigma_{Cp}}^2$ against *F*.

- Type 1, with dominant low frequency peaks at *F* of around 0.1 to 0.15 (figure 4a).
- Type 2, with similar low frequency peaks but also peaks at higher values of *F* frequencies of around 0.3 to 0.5 (figure 4b).
- Type 3, which were broad banded, with no indication of peaks or with a number of peaks throughout the frequency range (figure 4c).

For any particular configuration, any of the three distinct types could occur, which makes the use of ensemble averaging inappropriate in this case. Also figure 11 below, shows how the spectral type can vary along the platoon for individual runs. This will be discussed further in section 3.5.

The existence of different types of spectrum having thus been recognised, each individual spectrum was then allocated into one of the three types. This had to be done manually, and whilst the large majority of the spectra fell obviously into a distinct category, for a very small minority on the border between types 2 and 3 a degree of subjective judgment was involved. Although this needs to be borne in mind in what follows, any mis-categorisation of individual spectra is unlikely to significantly affect the results that follow.

The general statistics for the differential pressure coefficient spectra are indicated in table 1. It can be seen that the number of spectra for each vehicle spacing was large with 377 for *s* = 0.5, 415 for *s* = 1.0 and 521 for *s* = 1.5. The percentage of type 1 spectra, with the low

frequency peak, is greatest for the closest spacing of s = 0.5 (46%) and least for the greatest spacing of s = 1.5 (21%). The percentages of type 2 does not change greatly with vehicle spacing, whilst the percentage of spectra with no peak increases with spacing. Table 1 also shows the total percentage of spectra with a low frequency peak (Type 1 + Type 2).

s	0.5	1.0	1.5
Total number of spectra	377	415	521
% Type 1	46	36	21
% Type 2	19	19	19
% Type 3	35	45	60
% with low frequency peak (Type 1 + Type 2)	65	55	40

Table 1 General statistics of differential pressure spectra

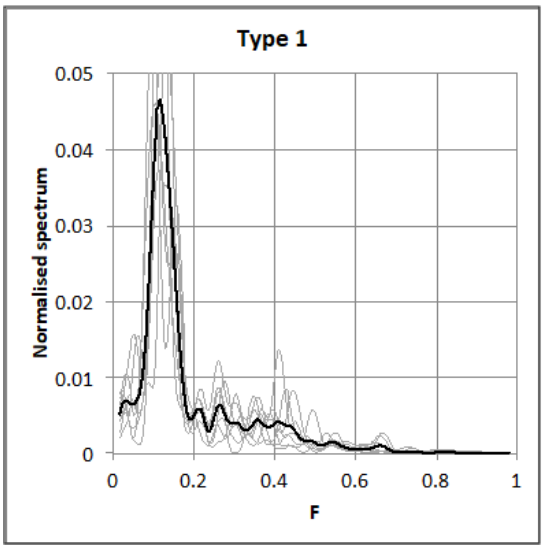

(a) Lorry 4, *s* = 0.5, tapping pair A

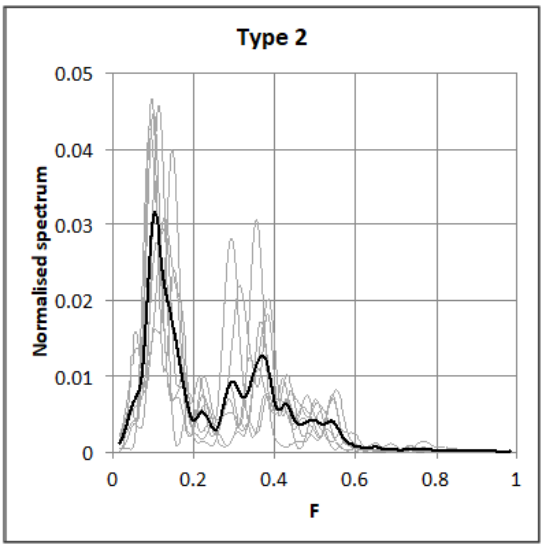

(b) Lorry 4, *s* = 0.5, tapping pair A

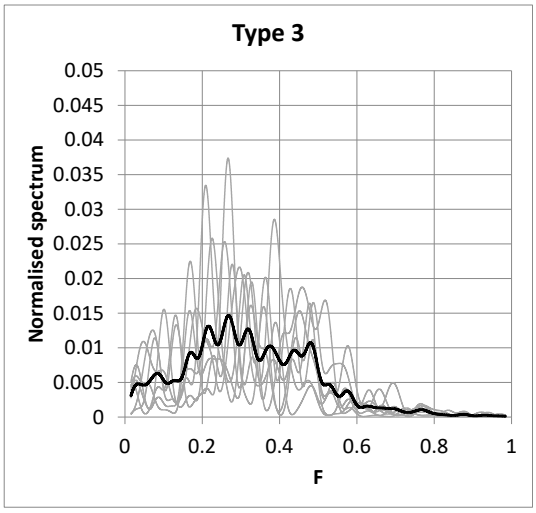

(c) Lorry 2, *s* = 1.5, tapping pair C

Figure 4 Different types of differential pressure spectra

(grey lines indicate spectra from individual runs, black lines average values)

3.2 Magnitude of unsteady pressure coefficients

Figure 5 shows the average standard deviations of unsteady differential pressure for each configuration. This data thus includes runs with spectra of all the different types. The results are very consistent, with pressure tap pair A, at the front of the box, having larger values for all lorries and spacings than pairs B and C. The values for the leading vehicle are higher than those for the others, which are generally very similar. The values for an isolated vehicle, not in a platoon, are very similar to those for the Lorry 1 case and are not shown in figure 5 for the sake of clarity. To give some context to these measurements, the reader is referred to the uncertainty analysis presented in Robertson et al (2019). This indicated the uncertainty of mean pressure coefficients at specific tappings was of the order of ± 0.05.

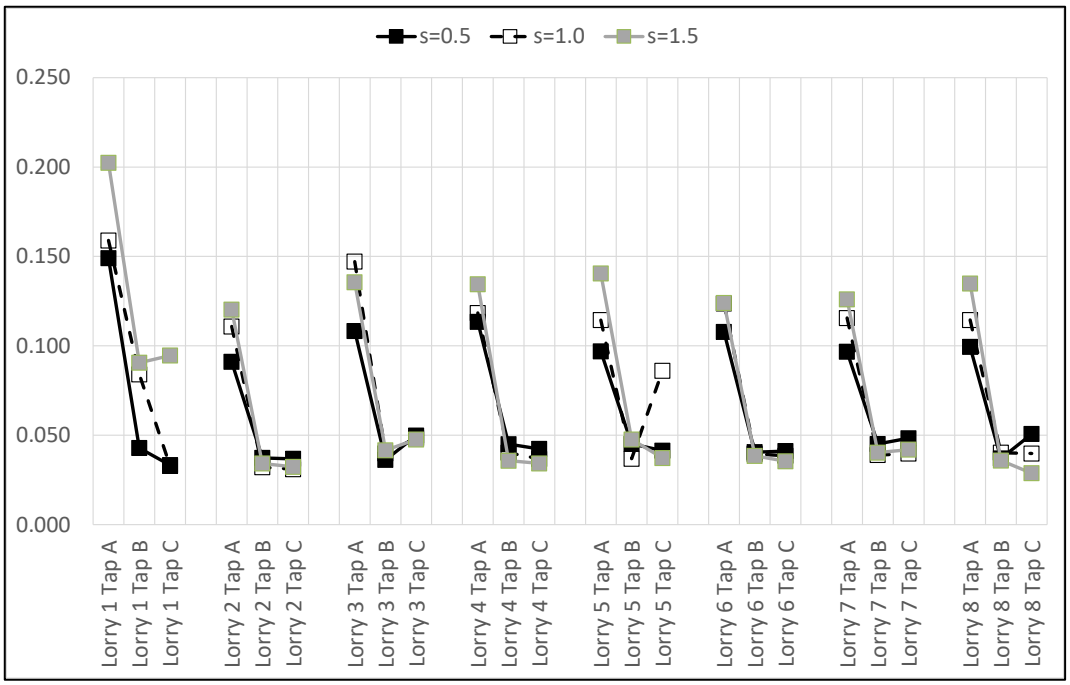

Figure 5 Standard deviation of unsteady differential pressure coefficient

3.3 Occurrence ranges of spectra of different types

Figures 6 to 8 show the percentages of spectra with low frequency peaks, with high frequency peaks, and with no peaks for each configuration tested. There were between 15 and 20 individual runs for each configuration. For the low frequency peaks (figure 6), the percentage for lorries 2 to 8 is very similar for a specific spacing, and well above the values for lorry 1. The percentage values for lorries 2 to 8 are higher for low vehicle spacings with average values of 72% for *s* = 0.5; 59% for *s* = 1.0 and 44% for *s* = 1.5. For the high frequency peaks (figure 7) the percentage for lorries 2 to 8 for all spacings is similar – 24% for *s* = 0.5; 24% for *s* = 1.0; and 31% for *s* = 1.5. For the no peak values (figure 8), the percentages show the reverse trend of those for the low frequencies – 26% for *s* = 0.5; 37% for *s* = 1.0; and 46% for *s* = 1.5. Again, the percentage occurrences for low and high frequency and broad banded spectral types for an isolated vehicle are very similar to those for the Lorry 1 case and are not included here.

The percentage figures thus tell a consistent story, but the uncertainties (due to the relatively small number of spectra for type 2 in particular) are around +/- 10% and this figure needs to be borne in mind when considering the results shown.

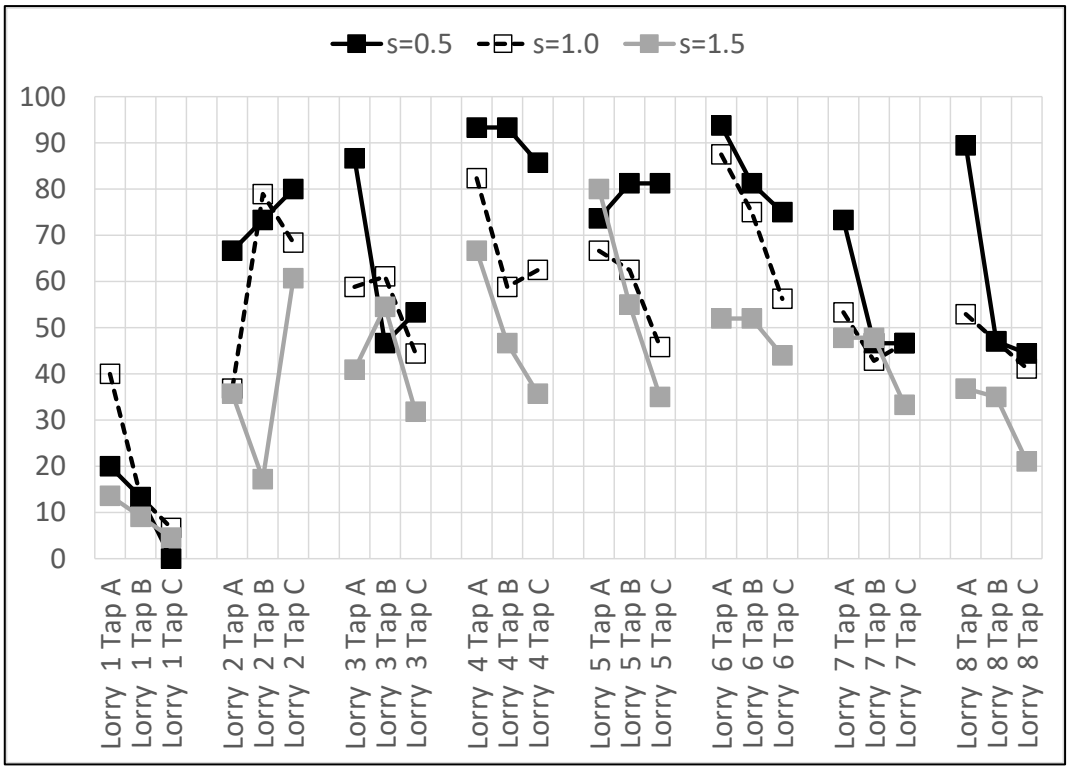

Figure 6 Percentages of low frequency peaks (type 1 and type 2)

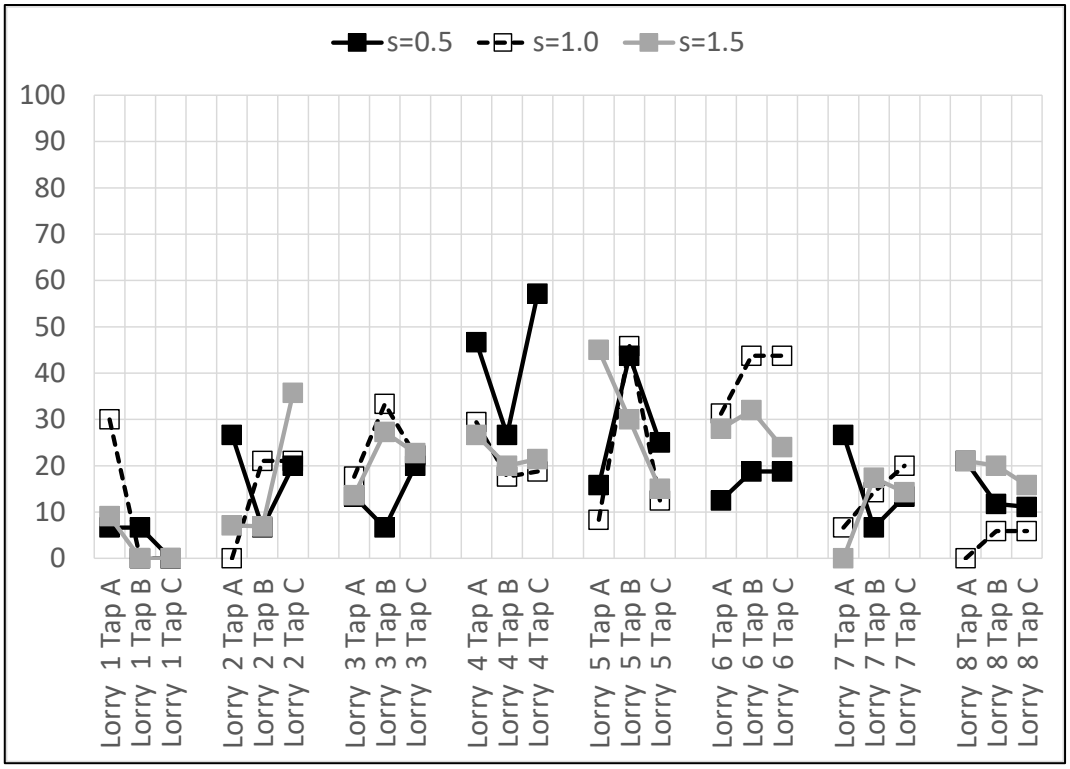

Figure 7 Percentages of high frequency peaks (type 2)

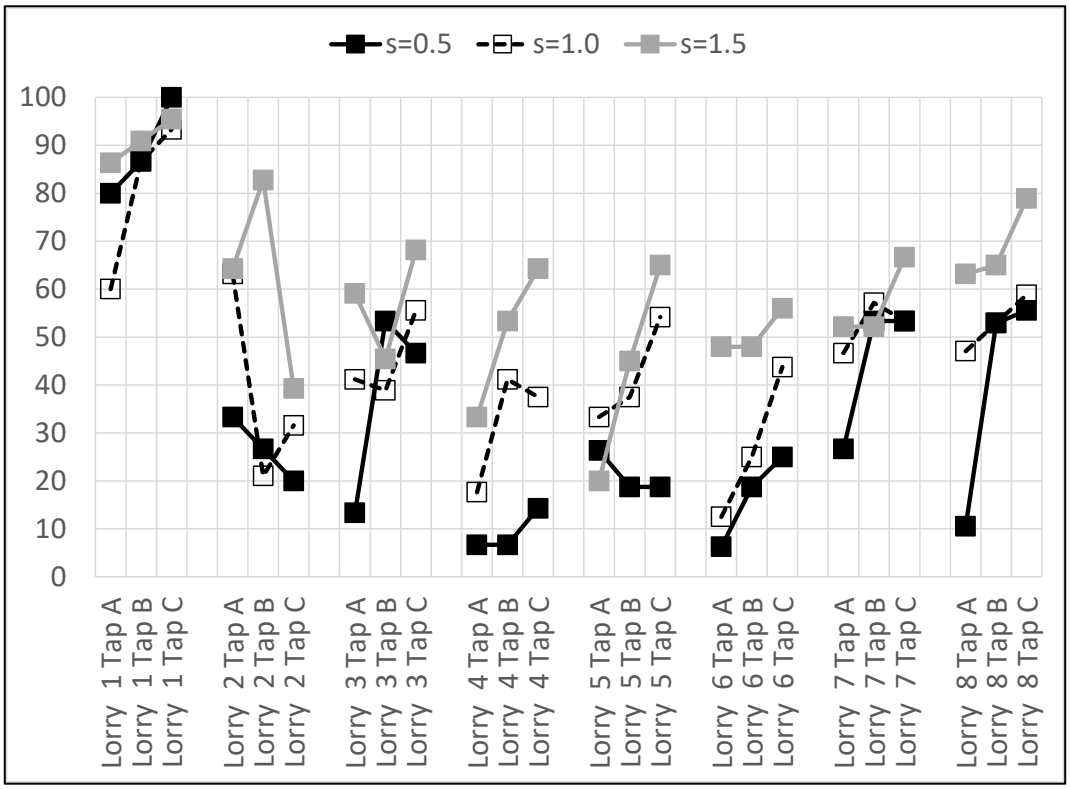

Figure 8 Percentages of broad banded spectra (type 3)

3.4 Frequencies of peaks

Figure 9 shows the values of F for the low frequency peaks (F_l) for all cases, and figure 10 shows a similar figure for the high frequency peaks (F_h). The standard errors for the former are of the order of 0.01, whilst for the latter they are of the order of 0.05, the latter reflecting the much smaller number of occurrences of high frequency spectra, and their rather variable nature. The values of F_l for all spacings are similar, with a fall along the platoon from a value of around 0.15 to a value of around 0.1. There is some indication that the values for s = 1.5 are rather lower than for the other s values, but any such effect is small. The values of F_h are constant at around 0.4 for all cases.

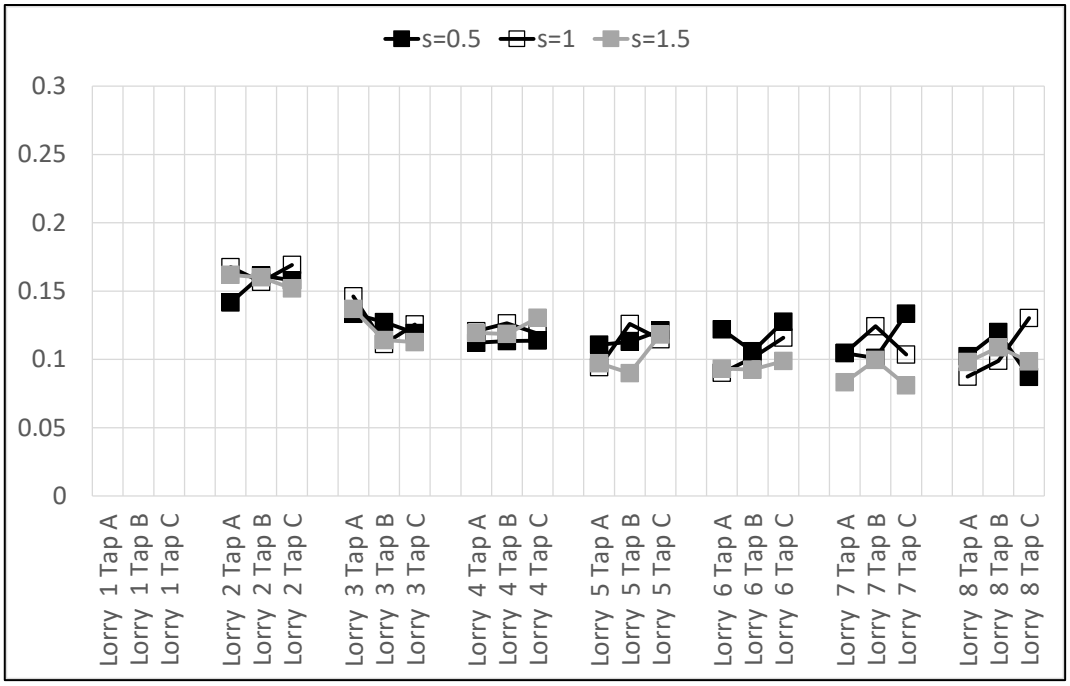

Figure 9 Values of F for low frequency peaks F_l

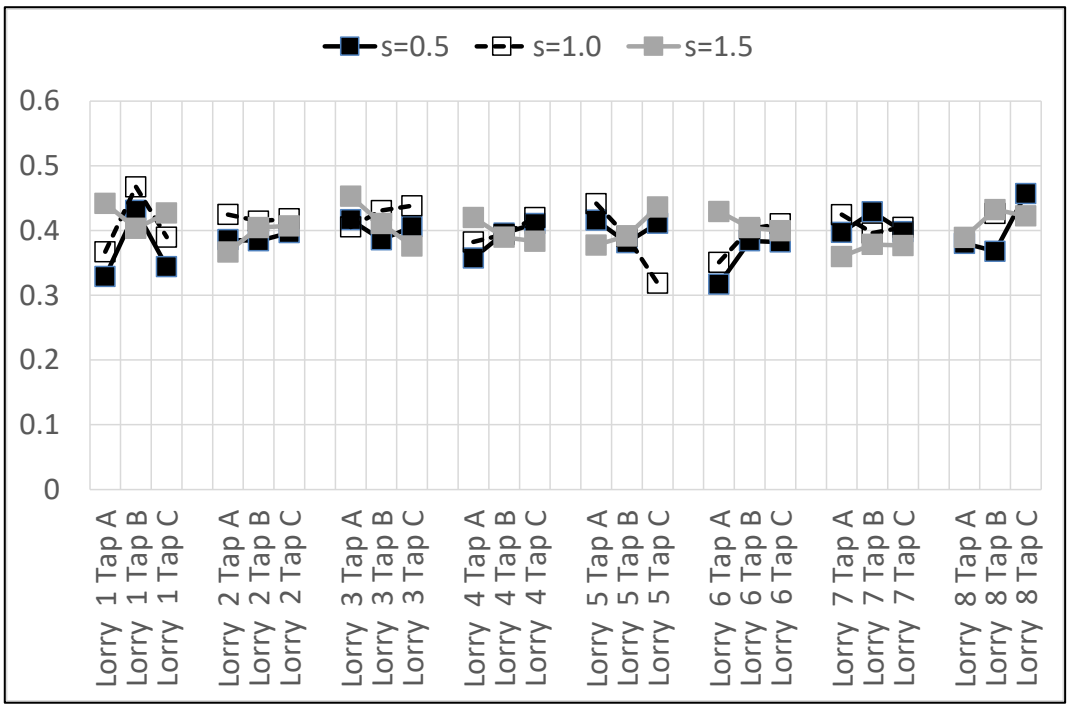

Figure 10 Values of F for high frequency peaks F_h

3.5 Persistence of spectral peaks

The question now arises as to the persistence of different types of spectra down the platoon during specific runs i.e. in any one run is the spectral type the same for all lorries in the platoon or does it vary from lorry to lorry. In principle this can be investigated by looking at spectra from different lorries for the same run on the TRAIN rig. However, as was pointed out above, space limitations within the lorry models made it impossible to measure all pressure tappings simultaneously. In addition, a range of experimental issues resulted in gaps in the data, where the pressure system within any one lorry failed on a small number of runs. Thus the data here is not as complete as would be wished. Nonetheless there are runs where the pressures are available on the majority of lorries from one individual run of the rig. Figure 11 shows the spectral types for these runs for the three vehicle spacings for tapping pair A only. Only those runs with the pressures measured on 5 or more lorries are shown – there is of course data from other runs that were used to obtain the statistics of spectral types and peak frequencies set out above. For each spacing there are between 10 and 14 runs that meet this criterion. The broad point to emerge from this figure is that for any one run, the smallest spacing (s = 0.5) shows that the low frequency peak (type 1 and type 2 spectra) persists over a number of lorries on many occasions. For the widest spacing of s = 1.5 there is much less persistence, with type 3 (broad banded) spectra becoming increasingly common. The results for s = 1.0 lie between those for s = 0.5 and s = 1.5.

An example of this persistence is shown in figure 12, for *s* = 1.0, run b. For lorries 1 and 2, the spectra are type 3, and show no peaks. The low frequency peak begins to be visible at lorry 3, and develops to a sharp peak by lorry 5, and then decays, so that for lorries 7 and 8 no peak can be seen. There is a hint on lorry 4 of the existence of a high frequency peak too, but this does not persist along the platoon. This development and decline is of considerable interest.

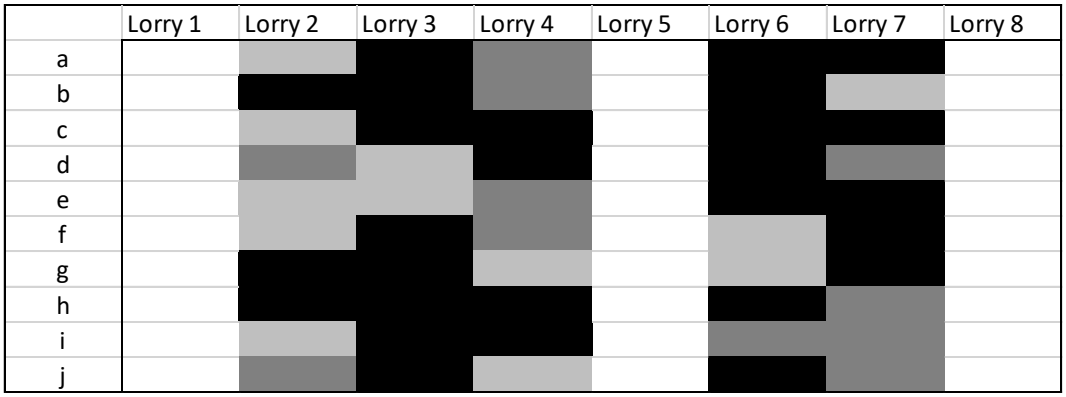

a) $s = 0.5$

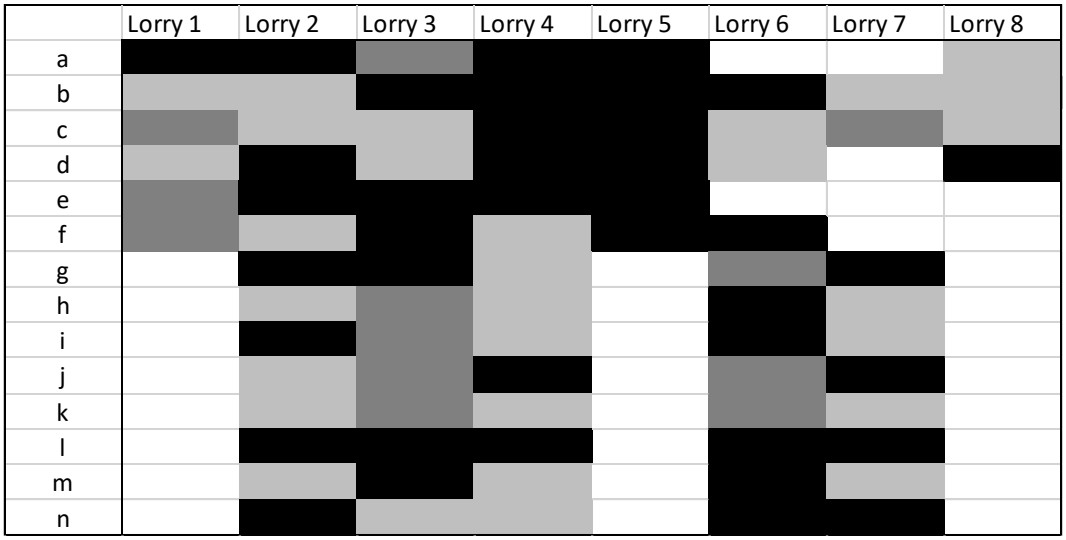

b) $s = 1.0$

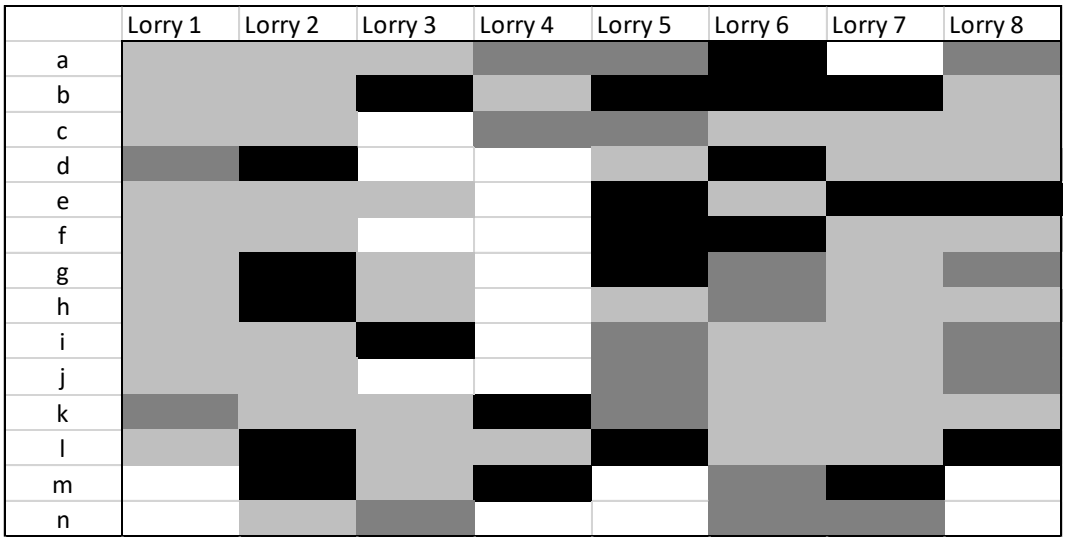

c) $s = 1.5$

Figure 11. Persistence of spectral types for tapping pair A

(Run identifier on left hand side. Shaded cells indicate where data is available. Black shading - type 1; Dark grey shading - Type 2; Light grey shading - Type 3)

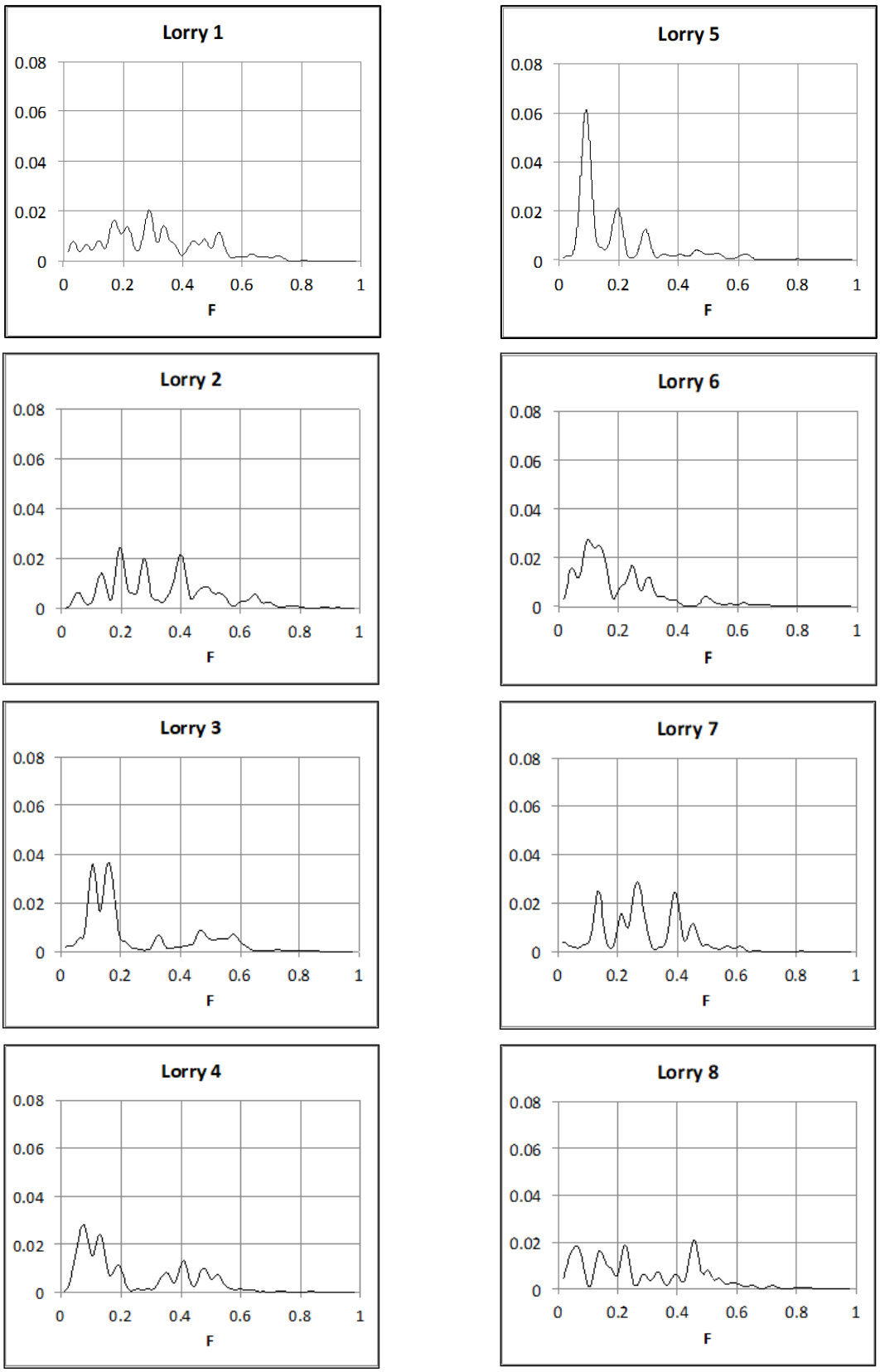

Figure 12 Normalised spectra for tapping pair A, *s* = 1.0, Run b

4. Wavelet analysis

To take forward the investigation into the unsteady flows measured in the experiments, we now turn to the results of a wavelet analysis of the velocities measured by a stationary probe as the platoon passes. We use data from the probe position shown in figure 3, which is close to the pressure tapping position on the passing platoon lorries. Before considering the results themselves, it is useful to firstly consider what they might show. Wavelet analysis gives a three-dimensional plot of wavelet power against dimensionless time and wavelet scale, the latter being the inverse of the Fourier frequency of the normal power spectra. For the sake of consistency with the results of the last section, we will define this axis in the wavelet plot by the non-dimensional frequency *F*. As the measurements are made as a platoon passes, it may be expected at the outset that peaks in wavelet power might be expected at two values of *F*. The first would arise from the varying large scale fluctuations as the entire platoon passes by with a characteristic frequency of $\frac{V}{\epsilon L_p}$ where L_p is the platoon length and ϵ is a factor greater than unity that allows for the length of the wake. In dimensionless terms $F_p = \frac{W}{\epsilon L_p}$. For the eight-lorry platoon, assuming $\epsilon = 2$, with $s = 0.5$, $F_p = 0.019$. We might also expect a peak of wavelet power at a frequency corresponding to the passing of an individual vehicle $V/L(1+s)$ with the dimensionless value given by $F_v = W/L(1+s)$. For $s = 0.5$, this gives a value of $F_v = 0.21$. We would also expect peaks in wavelet power corresponding to the two frequencies identified in the last section, F_l and F_h. However, F_l and F_h were measured in the plane of reference of the vehicle. If we assume that the oscillations at these frequencies are caused by waves passing down the platoon, one would expect that the frequencies experienced by an observer on the platoon would be different from those experienced by a stationary observer. To consider this further, let us assume that the velocities and pressures around the platoon, in the moving frame of reference are given by functions of the form

$$f = \bar{f} + f' sin\left(2\pi\left(\frac{x}{\Lambda} - \frac{t}{\mathrm{T}}\right)\right)$$

where $\bar{f}$ and f' are mean and fluctuating values of a generalised flow function. Here Λ is the wavelength of the function and T is the period. Since the normalised frequency is given by $F = \frac{W}{v\mathrm{T}}$ we can write this as

$$f = \bar{f} + f' sin\left(2\pi\left(\frac{x}{\Lambda} - \frac{Fv}{W}t\right)\right)$$

Now to relate this to the ground frame of reference we write $x = vt$ and thus

$$f = \bar{f} + f' sin\left(2\pi\left(\frac{v}{\Lambda} - \frac{Fv}{W}\right)t\right)$$

This represents an oscillation in time alone with a normalised frequency of $F' = \frac{W}{v}\left(\frac{v}{\Lambda} - \frac{Fv}{W}\right)$

From this we can obtain the relation $\frac{\Lambda}{W} = \frac{1}{F'+F}$. Thus, if identifications can be made between peaks in the moving and stationary frames of reference, this equation will allow an estimate to be made of the wavelength of the oscillation. This will be seen to be useful in what follows.

Now let us consider the experimental results themselves. As with the pressure measurements, these were found to be very variable from run to run, and the use of ensemble analysis was not appropriate. Figure 13 shows the results from one specific run of the rig for *s* = 0.5. It is not possible to describe any particular run as "typical" because of the

inter-run variability, but this set of data does show reasonably clearly the major features that were observed. Figure 13a shows a wavelet plot of the data for longitudinal velocity. Wavelet power is plotted against τ and the normalised frequency *F*, the latter being the inverse of wavelet scale. High values of wavelet power can be seen at low values of F, corresponding to the platoon passing frequency F_p discussed above. These values are around the value of F_p of 0.02 suggested above. A further peak in the wavelet spectrum can be discerned at around $F = 0.06$, which extends for the length of the platoon and into the wake. Smaller, less well-defined peaks can be seen at larger values of F. Note that figure 13a does not show any indication of a well-defined peak at the postulated vehicle passing frequency $F_v = 0.21$. Figures 13b shows a similar figure for the lateral velocity wavelet analysis for *s* = 0.5. The same features can be seen. Again, there is no indication of significant energy at the vehicle passing frequency. There is perhaps an indication at high frequencies on both plots of small peaks that are associated with the passage of individual vehicles.

Figures 13c and d show plots of the wavelet spectra for longitudinal and lateral velocities at normalised times corresponding to the passage of the centre of each of the lorries in the platoon. The low frequency platoon passing peak can be clearly seen to the left of the graph, and a well-defined peak is also visible for all lorries at around 0.04. Smaller, less well-defined peaks can be seen at around F = 0.2 to 0.25. These features are, to some degree, evident in all the wavelet spectra that have been analysed for all three platoon spacings.

Table 2 shows the average and standard deviation values of the frequencies of the low and high frequency peaks and the percentage of runs in which they occur, for all three vehicle spacings. It can thus be seen that the frequencies of the peaks are quite variable, with the standard deviations being quite large. The value of the standard deviation for the high frequency oscillation at s = 0.5 is significantly higher than for the other spacings. The reason for this is not clear. There is an indication that the peak frequencies decrease somewhat with increasing vehicle spacing, but the variation is within the standard deviation bands of the samples and the relatively small number of runs needs to be borne in mind. The low frequency peaks occur more frequently than the high frequency peak, and were in general much better defined. Thus, it does not seem unreasonable to identify these two peaks with the low and high frequency peaks of section 3, where it was shown that the low frequency peak is much better defined and occurs more often than the high frequency one. Notice that, in this data, they are at significantly lower values of F due to the change in the frame of reference i.e. $F_l' = 0.06$ against $F_l = 0.10$ and $F_h' = 0.18$ against $F_h = 0.4$. Putting these values into the relationship for wavelength derived above we can obtain estimates of the wavelengths of these two oscillations of $\Lambda_l = 6.2W$ and $\Lambda_h = 1.7W$. As $\frac{L}{W} = 3.2$, it can be seen that the wavelength of the low frequency oscillation is around 2 vehicle lengths and that of the high frequency oscillation is around half a vehicle length.

	Low frequency peak			High frequency peak		
s	Mean *F*	SD of *F*	% occurrence	Mean *F*	SD of *F*	% occurrence
0.5	0.060	0.017	75	0.184	0.049	60
1.0	0.058	0.013	65	0.152	0.016	35
1.5	0.048	0.018	65	0.148	0.020	35

Table 2 Low and high frequency peaks from wavelet analysis

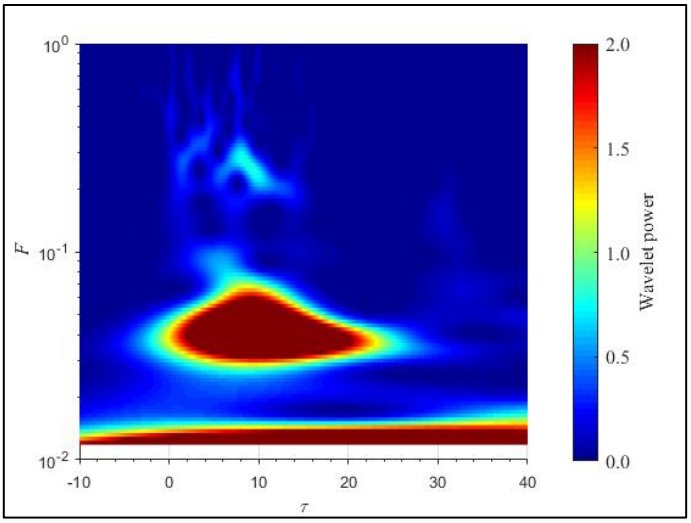

a) Longitudinal velocity wavelet plot

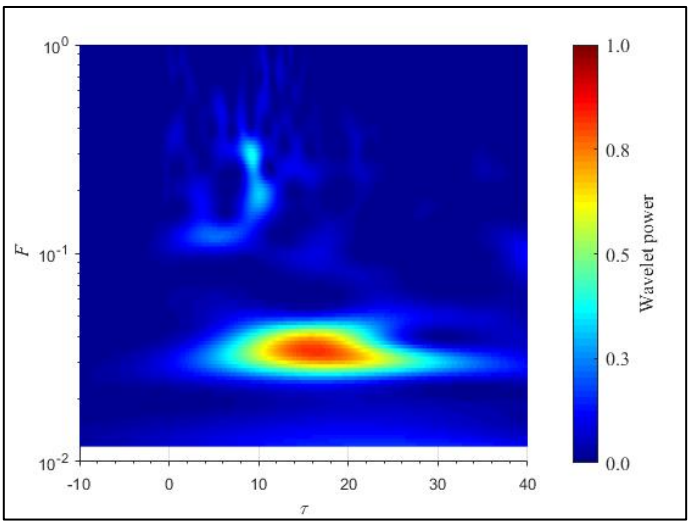

b) Lateral velocity wavelet spectra

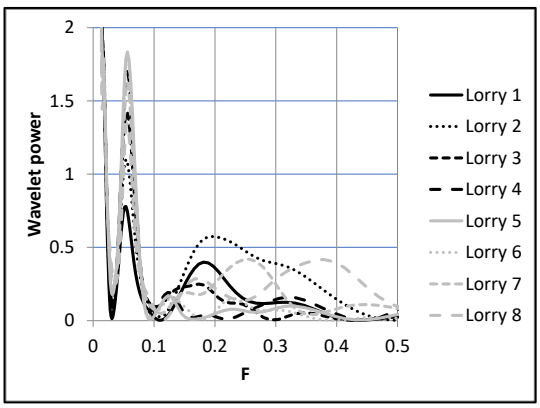

c) Longitudinal velocity wavelet plot

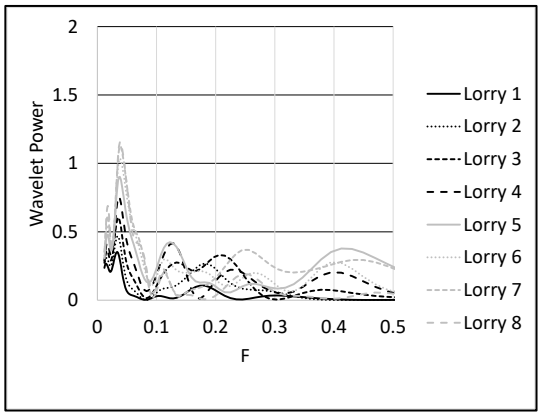

d) Lateral velocity wavelet spectra

Figure 13. Wavelet analysis for $s = 0.5$

5. Discussion

The experimental results clearly indicate several modes of flow along the platoon, with low and high frequency spectral peaks, and also broad banded spectra. Although there is some persistence of these types along the platoon for any one run, there is much variability, and the spectral type can change, more than once, along the platoon. The question thus arises as to the nature of this unsteadiness. At this point it is worth summarising what the experimental results tell us.

- The unsteadiness is greatest towards the front of the lorry box.
- The low frequency peak occurs less frequently on the front lorry than on other lorries in the platoon.
- This peak occurs most frequently on spectra for $s = 0.5$, and least frequently for $s = 1.5$.
- The normalised frequency of this peak, F_l falls from around 0.15 on lorry 2 to around 0.10 on lorry 8. It is not significantly affected by the platoon spacing.
- The high frequency peak occurs on all lorries, at about the same percentage occurrence rate for all spacings.
- The normalised frequency of this peak, F_h is close to 0.4 for all vehicle spacings.
- The wavelet analysis of the velocity next to the platoon also shows these high and low frequency peaks, again, with significant variability in the frequency and magnitude of these peaks.
- These results show that the low frequency oscillation has a wavelength of around two vehicles length, and tends to persist along the length of the platoon and into the wake. The high frequency oscillation has a wavelength of about half a vehicle length, and is more restricted spatially.

Now consider the analysis of He et al (2019). They carried out DDES calculations for the 8-vehicle platoon studied here at a spacing of *s*=0.5, and the results of these calculations are useful in interpreting the experimental results discussed in this paper. Figure 14 below shows the velocity profiles measured along the side of the lorry trailers and 14b shows the streamwise turbulence intensity. The main point to emerge from these results is that on lorry 1 there is a clearly defined separated flow at the front of the trailer side, with a high turbulence intensity. For lorries 2 to 8, this separation is much less noticeable, if it exists at all, and a boundary layer can be seen to develop along the platoon, with similar velocity and turbulence intensity characteristics for all lorries.

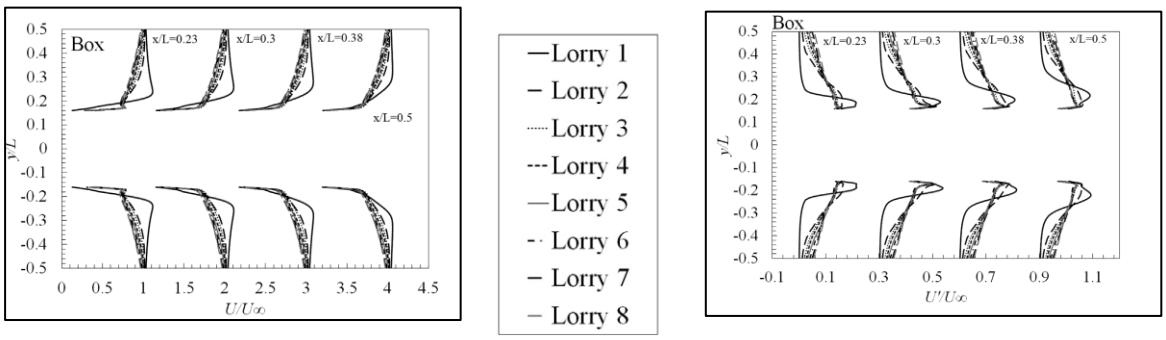

(a) Velocity profiles along trailer

b) Turbulence intensity profiles along trailer

Figure 14. Results of DDES calculations (from He et al, 2019)

(*x* axis is mean or standard deviation of flow velocity normalised with vehicle velocity; *y* axis is lateral distance from platoon centreline; curves are shown at different points along the box of the lorry, normalised by vehicle length. Successive profiles are shifted along the x-axis by 1 unit for the mean and 0.3 units for the standard deviation.)

He et al (2019) also calculated the spectra of fluctuating side force on vehicles in the platoon, and for all except lorry 1, they showed a peak at a value of F of around 0.1 to 0.15. The calculated frequencies are compared with the frequencies of the low frequency oscillation at tap A in figure 15. The agreement can be seen to be remarkably good. Note that tap A contains the majority of the variance of the fluctuations along the trailer and the pressures at this point can be expected to dominate the fluctuating side force. Now, it was also possible to calculate the overall side force on the lorry box for some lorries, by taking the weighted averages of the time histories of the pressures at the three tap positions. The approximate nature of these values must be stressed as they were only calculated from a very small number of tapping pairs. The standard deviation of the side force coefficient (based on vehicle frontal area) are compared with those of He et al in figure 16. It can be seen that the experimental results lie well above the calculated results, which is consistent with the fact that the DDES calculations only appear to model one mode of unsteadiness, and thus do not capture the entirety of the unsteady flow.

It would thus seem that we can conclude that the flow patterns calculated by He et al (2019) are representative of the low frequency oscillations found in the experimental results. The calculations however do not show the overall complexity of the experiments, and only describe one of several modes of flow, albeit possibly the most significant. The experimental data shows a switching between different unsteady modes that is not replicated in the calculations.

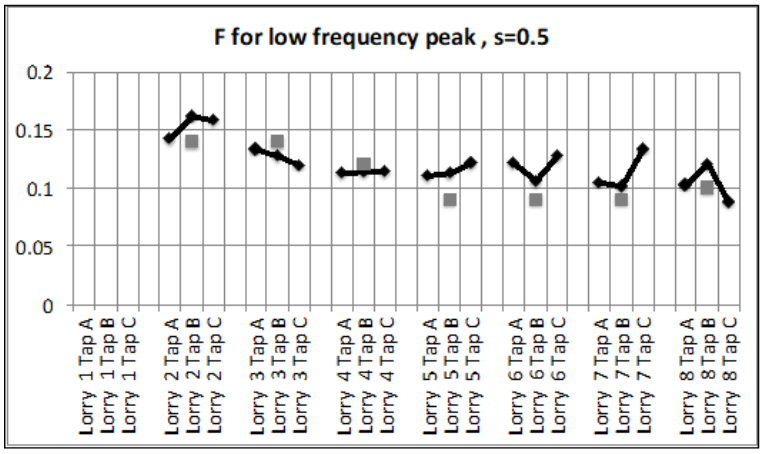

Figure 15. Comparison of low frequency peak values with calculations of He et al (2019)

(grey squares indicate calculated values)

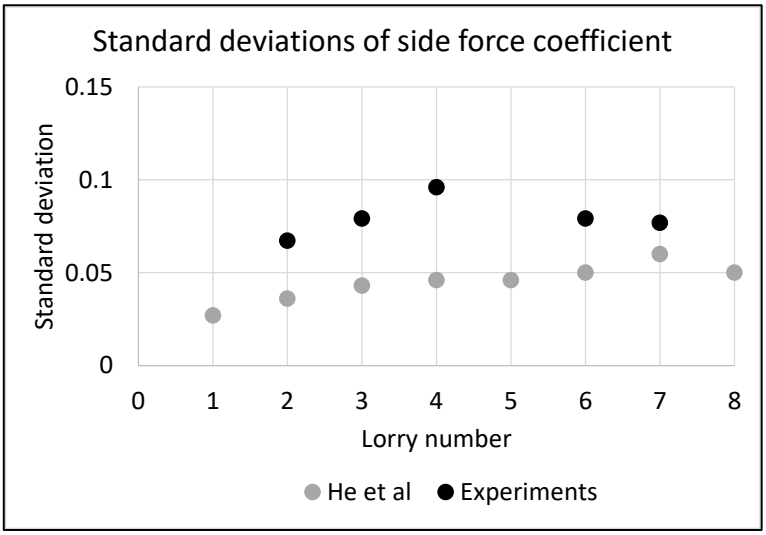

Figure 16. Comparison of side force coefficient standard deviations with the calculations of He et al (2019)

On the basis of the experimental and computational results it can thus be hypothesised that the low frequency oscillation is an oscillation of the flow around at least a significant proportion of the platoon, with a wavelength of several vehicle lengths, and a general persistence along the platoon and in the wake. This seems to be fed by the separated flow between the vehicles in the platoon and is strongest at the front of each lorry. The simple sinusoidal model used to determine the wavelength cannot be wholly correct, as the frequency of this oscillation varies along the length of the platoon. Figure 6 shows that the percentage of runs that this oscillation occurs changes with platoon spacing, which again suggests that it is a platoon rather than an individual vehicle affect.

The high frequency oscillation is by contrast much more localised, with a wavelength of half a vehicle length, and is more intermittent in nature. The frequency of this oscillation stays constant, within wide bounds, regardless of vehicle spacing or distance along the platoon, and the percentage of runs for which it occurs also remains constant (figure 7). This suggests

that this oscillation is due to localised effects on each lorry – either due to a wake instability in the gap upstream of the lorry (although one might expect the frequency to vary with lorry spacing if this were the case) or, and this is more likely, due to some sort of separated shear layer instability.

To assess the practical implications of this unsteadiness, the equivalent full-scale values of oscillation frequency and side force standard deviation need to be calculated from the dimensionless values given above. Assuming that the average side force coefficient standard deviation is 0.08 from figure 16, for the equivalent vehicle at full scale and travelling at 25m/s, this gives a standard deviation of side force of 260 N. From this figure one might expect around half of this figure to be due to the low frequency oscillation and around half due to the high frequency oscillation. The equivalent full-scale frequency for the former is around 1 Hz and for the latter is around 4 Hz.

The question then arises as to the significance of this value of oscillating force. Whilst this is difficult to judge without a full dynamic calculation of vehicle / aerodynamics / driver behaviour, some indication can be given by considering the magnitude of the oscillating forces in comparison to those caused by steady crosswind forces. One might expect that the peak value of the oscillating forces would be around three times the standard deviation - say around 800N. Now using data from Sterling et al (2010) this corresponds to the steady side force caused by a pure crosswind of around 3m/s for a vehicle of the same geometry as tested here travelling at 25m/s. 3m/s is around the average UK wind speed at this height above the ground. A strong wind of 10 m/s at 10m above ground (the definition of a strong wind) would produce steady forces of 2300N, which is still well below the value required to overturn the vehicle. Thus, in these terms, the oscillating forces are not large, but note that the time scale of cross wind forces is much longer than the unsteady forces described here, which will be close to natural frequencies of the vehicle system. It is likely that the effects of such forces, if they can be shown to exist at full scale, will be predominantly to increase driver fatigue rather than causing a safety hazard. In a similar way, if platoons of lorries are autonomously controlled in the future, then the autonomous control system must be able to correct for oscillatory lateral forces close to the natural frequencies of the vehicle dynamic system, which could pose something of a design challenge.

6. Conclusions

This paper presents for the first time a detailed analysis of the unsteady forces experienced by lorries travelling in a close proximity platoon formation. From the results of the investigation described in the preceding sections the following important conclusions can be drawn.

- The moving model TRAIN Rig has been shown to be a viable tool for the investigation of unsteady flows around platoons, and allows long platoons to be studied with a correct ground simulation.
- The flow around the platoon displays considerable unsteadiness and intermittency. The latter makes ensemble averaging techniques unusable, and the results need to be considered on a run by run basis.
- In both the pressure measurements on lorries in the platoon, and the velocity measurements along the side of the platoon, two types of unsteadiness can be detected.
- The first is a strong low frequency oscillation with a wavelength of several vehicle lengths and can be considered as an unsteadiness of the overall platoon flow field.
- The second is a higher frequency unsteadiness, with a wavelength of around half a vehicles length, that is probably due to a shear layer instability on individual vehicles in the platoon.
- These two types of unsteadiness are both transitory, although the former is more common, and can persist over a number of vehicle lengths in the platoon.
- DDES calculations pick out the low frequency unsteadiness well, and the predicted frequencies are close to the experimental values. However, these calculations do not show the high frequency oscillation at all. It thus seems that only one of several modes of flow is captured by these calculations.
- The standard deviation of the low frequency oscillations of side force on a full-scale lorry travelling at 25m/s has been calculated to be around 260N at dominant frequencies of 1 to 4Hz. The peak values of these unsteady forces are well below those produced by strong steady cross winds, but, as the frequencies are close to those that might be expected in the dynamic vehicle / driver system, may well result in increased driver fatigue in platoon formation. Before any firm conclusions of this type can be arrived at however, the existence of such oscillations at full scale needs to be demonstrated.

As noted in section 1, experiments have also been carried out to measure the steady and unsteady pressures on “Windsor” vehicles and close running trains. It remains to be seen if these vehicle configurations exhibit similar unsteady behaviour.

Acknowledgements

The current work is carried out on an EPSRC funded project entitled 'The aerodynamics of close running ground vehicles - EP/N004213/1'. Wavelet software as used in Torrence & Compo, 1998 is available at URL: http://paos.colorado.edu/research/wavelets/

References

Baker, C. J., Dalley, S. J., Johnson, T., Quinn, A., & Wright, N. G. (2001). The slipstream and wake of a high-speed train. Proceedings of the Institution of Mechanical Engineers, Part F: Journal of Rail and Rapid Transit, 215 (2), 83-99.

BBC News. (2017). 'Self-driving' lorries to be tested on UK roads. Retrieved August 2020 from https://www.bbc.co.uk/news/technology-41038220

Bruneau, C.-H., Khadra, K., & Mortazavi, I. (2017). Flow analysis of square-back simplified vehicles in platoon. International Journal of Heat and Fluid Flow, 66, 43-59.

Chan, E. (2012). Overview of the SARTRE Platooning Project: Technology Leadership Brief. SAE Technical Paper 2012-01-9019.

CORDIS. (2012). Periodic Report Summary 2 - SARTRE (Safe road trains for the environment; developing strategies and technologies to allow vehicle platoons to operate on normal public highways. Retrieved August 2020 from https://cordis.europa.eu/result/rcn/58617_en.html

Davila, A., Aramburu, E., & Freixas, A. (2013). Making the best out of aerodynamics: Platoons. SAE Technical paper 2013-01-0767.

Department for Transport, Highways England, and Centre for Connected and Autonomous Vehicles. (2017). Green light for lorry 'platooning'. Retrieved August 2020 from https://www.gov.uk/government/news/green-light-for-lorry-platooning

Ebrahim, H. (2018). Analysis of the surface pressure and power consumption experienced by full-scale vehicles in platoon. Proceedings of the Institution of Mechanical Engineers International Conference on Vehicle Aerodynamics.

Ebrahim, H., & Dominy, R. (2020). Wake and surface pressure analysis of vehicles in platoon. Journal of Wind Engineering & Industrial Aerodynamics, 201, 104144.

Fallah, S. (2018). We're not ready for driverless cars. Retrieved August 2020 from https://www.weforum.org/agenda/2018/04/driverless-cars-are-forcing-cities-to-become-smart/

Goldin, P. (2018). 10 advantages of autonomous vehicles. (ITSdigest) Retrieved August 2020 from http://www.itsdigest.com/10-advantages-autonomous-vehicles.

Grandemange, M., Gohlke, M., & Cadot, O. (2013). Turbulent wake past a three-dimensional blunt body. Part 1. Global modes and bi-stability. Journal of Fluid Mechanics, 722, 51-84.

He, M., Huo, S. R., Hemida, H., Bourriez, F., Robertson, F. H., Soper, D., et al. (2019). Detached eddy simulation of a closely running lorry platoon. Journal of Wind Engineering and Industrial Aerodynamics , 103956, 193.

Humphreys, H., & Bevly, D. (2016). Computational Fluid Dynamic Analysis of a Generic 2 Truck Platoon. SAE Technical Paper 2016-01-8008.

Iliaifar, A. (2013). Lidar, lasers, and logic: Anatomy of an autonomous vehicle. Retrieved August 2020 from Digital Trends: https://www.digitaltrends.com/cars/lidar-lasers-and-beefed-up-computers-the-intricate-anatomy-of-an-autonomous-vehicle/.

Katz, J. (2016). Aerodynamics of race cars. Annual Review of Fluid Mechanics, 38 (1), 27-63.

Lahaye, A., Leroy, A., & Kourta, A. (2014). Aerodynamic characterisation of a square back bluff body flow. International Journal of Aerodynamics, 4, 43-60.

Le Good, G., Resnick, M., Boardman, P., & Clough, B. (2018). Effects on the Aerodynamic Characteristics of Vehicles in Longitudinal Proximity Due to Changes in Style. SAE Technical Paper 2018-37-0018.

Manyika, J., Chui, M., Bughin, J., Dobbs, R., Bisson, P., & Marrs, A. (2013). Disruptive technologies: Advances that will transform life, business, and the global economy. McKinsey Global Institute.

Mcarthur, D., Burton, D., Thompson, M., & Sheridan, J. (2018). An experimental characterisation of the wake of a detailed heavy vehicle in cross-wind. Journal of Wind Engineering and Industrial Aerodynamics, 175, 364-375.

Mirzaei, M., & Krajnović, S. (2016). Large eddy simulations of flow around two generic vehicles in a platoon. In A. Segalini (Ed.), Proceedings of the 5th International Conference on Jets, Wakes and Separated Flows (ICJWSF2015), (pp. 283-288).

Pagliarella, R., Watkins, S., & Tempia, A. (2007). Aerodynamic Performance of Vehicles in Platoons: The Influence of Backlight Angles. SAE Technical Paper 2007-01-1547.

Robertson, F. H., Bourriez, F., He, M., Soper, D., Hemida, H., Sterling, M., et al. (2019). An experimental investigation of the aerodynamic flows created by lorries travelling in a long platoon. Journal of Wind Engineering and Industrial Aerodynamics, 193, 103966.

Schuetz, T. (2015) Aerodynamics of Road Vehicles, SAE, 5th edition.

Soper, D., Baker, C., & Sterling, M. (2014). Experimental investigation of the slipstream development around a container freight train using a moving model facility. Journal of Wind Engineering and Industrial Aerodynamics, 135, 105-117.

Soper, D., Gallagher, M., Baker, C., & Quinn, A. (2016). A model-scale study to assess the influence of ground geometries on aerodynamic flow development around a train. Proceedings of the Institution of Mechanical Engineers, Part F: Journal or Rail and Rapid Transit, 231 (8), 916–933.

Sterling, M., Quinn A., Hargreaves D., Cheli F., Sabbioni F., Tomasini G., Delaunay D., Baker C. and Morvan H. (2010). A comparison of different methods to evaluate the wind induced forces on a high sided lorry", Journal of Wind Engineering & Industrial Aerodynamics, 98, 10–20.

Torrence, C., & Compo, G. P. (1998). A practical guide to wavelet analysis. Bulletin of the American Meteorological Society, 79 (1), 61-78.

Tsuei, L., & Savaş, Ö. (2001). Transient aerodynamics of vehicle platoons during in-line oscillations. Journal of Wind Engineering and Industrial Aerodynamics, 89 (13), 1085-1111.

Vegendla, P., Sofu, T., Saha, R., Madurai Kumar, M., & Hwang, L.-K. (2015). Investigation of Aerodynamic Influence on Truck Platooning. SAE Technical Paper 2015-01-2895.

Volpe, R., Devinant, P., & Kourta, A. (2015). Experimental characterization of the unsteady natural wake of the full-scale square back Ahmed body: flow bi-stability and spectral analysis. Experiments in Fluids, 56, 99.

Watkins, S., & Vino., G. (2008). The effect of vehicle spacing on the aerodynamics of a representative car shape. Journal of Wind Engineering and Industrial Aerodynamics, 96 (6), 1232-1239.

Zabat, M., Stabile, N., Farascaroli, S., & Browand, F. (1995). The aerodynamic performance of platoons: A final report. UC Berkeley: California Partners for Advanced Transportation Technology.